Biomechanical analysis of four different medial row configurations of suture bridge rotator cuff repair

千住, 隆博

https://doi.org/10.15017/4060028

出版情報：Kyushu University, 2019, 博士（医学）, 課程博士
バージョン：

Clinical Biomechanics 69 (2019) 191–196

Contents lists available at ScienceDirect

Clinical Biomechanics

journal homepage: www.elsevier.com/locate/clinbiomech

Biomechanical analysis of four different medial row configurations of suture bridge rotator cuff repair

Takahiro Senju[a], Takamitsu Okada[a,*], Naohide Takeuchi[a], Naoya Kozono[a], Yoshitaka Nakanishi[a], Hidehiko Higaki[b], Takeshi Shimoto[c], Yasuharu Nakashima[a]

[a] Department of Orthopaedic Surgery, Graduate School of Medical Sciences, Kyushu University, 3-1-1 Maidashi, Higashi-ku, Fukuoka City, Fukuoka 812-8582, Japan
[b] Department of Life Science, Faculty of Life Science, Kyushu Sangyo University, 2-3-1, Matsukadai, Higashi-ku, Fukuoka City, Fukuoka 813-8503, Japan
[c] Department of Information and System Engineering, Faculty of Information Engineering, Fukuoka Institute of Technology, 3-30-1, Higashi-ku, Fukuoka City, Fukuoka 811-0295, Japan

ARTICLE INFO

Keywords:
Rotator cuff repair
Suture bridge technique
Medial row configuration
Type 2 retear
Biomechanical study

ABSTRACT

Background: Rotator cuff tendon rupture after suture bridge repair occasionally occurs at the medial row, with remnant tendon tissue remaining at the footprint. While concentrated medial row stress is suspected to be involved in such tears, the optimal suture bridge technique remains controversial.
Methods: This study aimed to investigate the construct strength provided by suture bridge techniques having four different medial row configurations using artificial materials (n = 10 per group): Group 1, four-hole (two stitches per hole) knotless suture bridge; Group 2, eight-hole (one stitch per hole) parallel knotless suture bridge; Group 3, eight-hole non-parallel knotless suture bridge; and Group 4, eight-hole knot-tying suture bridge. Each construct underwent cyclic loading from 5 to 30 N for 20 cycles, followed by tensile testing to failure. The ultimate failure load and linear stiffness were measured.
Findings: Group 2 had the highest ultimate failure load (mean 160.54 N, SD 6.40) [Group 4 (mean 150.21 N, SD 9.76, $p = 0.0138$), Group 3 (mean 138.80 N, SD 7.18, $p < 0.0001$), and Group 1 (mean 129.35 N, SD 4.25, $p < 0.0001$)]. The linear stiffness of Group 2 (mean 9.32 N/mm, SD 0.25) and Group 4 (mean 9.72 N/mm, SD 0.40) was significantly higher ($p = 0.0032$) than that of Group 1 (mean 8.44 N/mm, SD 0.29) and Group 3 (mean 8.61 N/mm, SD 0.31).
Interpretation: In conclusion, increasing the number of suture-passed holes, arranging the holes in parallel, and a knotless technique improved the failure load following suture bridge repair.

1. Introduction

The suture bridge technique (SBT) is a common technique for rotator cuff repair, which was introduced by Park et al. in 2006 (Park et al., 2006). Since then, suture bridge repair has come into general use and is associated with good clinical outcomes and improved tendon-bone healing (Gartsman et al., 2013; Neyton et al., 2013). Nevertheless, the retear rate after suture bridge repair is still as high as 10%–30% (Neyton et al., 2013; Park et al., 2010; Kim et al., 2012a; Hein et al., 2015; Kim et al., 2012b, 2018; Bedeir et al., 2019). In addition, Cho et al. (2010) reported that 74% of retears showed an unusual pattern of tendon failure where the tendon ruptured in the medial row while the footprint of the tendon remained well fixed to the greater tuberosity with a normal thickness; this is referred to as a type 2 retear. While concentrated medial row stress is suspected to be involved in such tears, the optimal medial row configurations of SBT are still controversial. Various types of medial row configurations of the SBT have been reported, and the construct strength of these techniques has been investigated in biomechanical studies using human cadaveric rotator cuff tendons or animal tendons (Anderl et al., 2012; Awwad et al., 2014; Barber et al., 2010; Maguire et al., 2011; Montanez et al., 2016; Park et al., 2014; Pauly et al., 2010, 2011; Wu et al., 2016; Zhang et al., 2018). However, these studies had several limitations in the biomechanical testing methods. When using human and animal tendons or bone, it is difficult to match the size and mechanical properties of the materials with accuracy. In addition, the retear pattern of the previous biomechanical studies was almost always a type 1 retear, with the sutures cutting through the tendon and nothing remaining on the footprint (Awwad et al., 2014; Barber et al., 2010; Maguire et al., 2011; Montanez et al., 2016; Park et al., 2014; Pauly et al., 2010, 2011; Wu

* Corresponding author.
E-mail address: t-okada@ortho.med.kyushu-u.ac.jp (T. Okada).

https://doi.org/10.1016/j.clinbiomech.2019.07.015
Received 14 December 2018; Accepted 15 July 2019

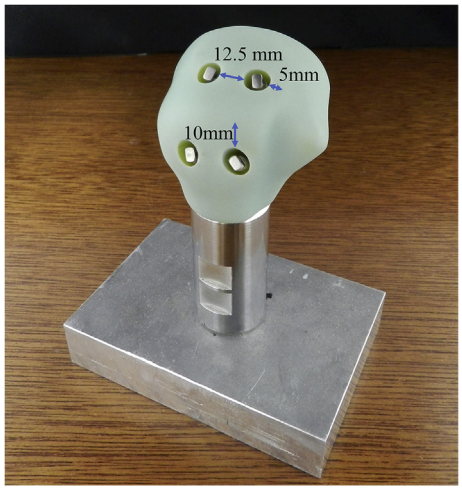

Fig. 1. Human proximal humerus bone model made using a 3D printer. The right shoulder from a healthy male subject was selected. Two medial anchors were inserted along the border of the articular surface, at the medial aspect of the greater tuberosity, 12.5 mm apart. Another two anchors were placed 10 mm distal to the edge of the greater tuberosity, also 12.5 mm apart. The humerus bone model was fixed to an iron pipe on a stand by a screw.

et al., 2016). Thus far, no studies have reported the failure mode of tensile testing exclusively for type 2 retears.

To address these limitations, we used artificial materials to biomechanically study suture bridge repair, which allowed us to accurately match the size, shape, and mechanical properties of the materials used in the study, such as tendon models and bone models. Furthermore, we chose the cuff model based on the results of a pilot study, whereupon the condition of the retear pattern after suture bridge repair consistently showed type 2 retear.

The purpose of this study was to investigate the construct strength of four different medial row configurations of suture bridge repair. This study may help to reduce the incidence of type 2 retear.

2. Methods

2.1. A three-dimensional (3D) bone model of the proximal humerus (Fig. 1)

The Institutional Review Board of Kyushu University (Fukuoka, Japan) approved this study. The right shoulder of a male with no symptoms of a rotator cuff tear and abnormal computed tomography (CT) and magnetic resonance imaging (MRI) findings was selected. First, using OsiriX (Pixmeo, Geneva, Switzerland), a 3D image of the humerus was formed based on the CT Digital Imaging and Communications Medicine (DICOM) data, which was converted to a Standard Triangulated Language (SLT) file. Subsequently, the surface of the 3D humerus was smoothed using Autodesk 123D design (Autodesk, Inc., San Francisco, California). Next, an Objet500 Connex 3D Printer (Stratasys Ltd.©, Minneapolis, MN) was used to construct a 3D bone model of the proximal humerus, which was made from an ABS-like (acrylonitrile, butadiene, styrene) resin material. Four screws with a notched post shape, named SAIPOK (MISUMI-VONA, Tokyo, Japan), which could thread the suture, were then used as anchors. Two medial anchors were inserted along the border of the articular surface, at the medial aspect of the greater tuberosity, 12.5 mm apart (Park et al., 2014). Another two anchors were placed 10 mm distal to the edge of the greater tuberosity, also 12.5 mm apart. The humerus bone model was fixed to an iron pipe on a stand by a screw.

2.2. The rotator cuff model

Silicon rubber sheets (Tigers Polymer Corporation, Osaka, Japan) were used for the rotator cuff model. A rectangular model of 36-mm width, 70-mm length, and 3-mm thickness was created. The 36-mm width was chosen to model a large cuff tear as per the classification of rotator cuff tears proposed by Cofield (Deolio and Cofield, 1984), and the thickness was selected based on a previous study (Goschka et al., 2015; Itoi et al., 1995). The material properties of the sheets from the pilot study were as follows: solidity, A70; ultimate tensile strength, 223.36 (SD 3.61) N, approximately 2.06 N/mm^2; elongation, 23.88 (SD 2.17) mm. The tensile strength of the silicone rubber used in the current study was measured at approximately 2.06 N/mm^2 in the pilot study. Sano et al. (1997) reported that as the degenerative changes increased, the ultimate tensile stress of the tendon decreased at the insertion area and the minimum ultimate tensile stress was approximately 2 N/mm^2. Therefore, we chose silicone rubber for the cuff model to match the tensile strength with predicted degenerated or torn rotator cuff tendons.

2.3. Repair techniques

The double-loaded sutures were used in all reconstruction techniques (in total, two strands were loaded to each anchor in the medial row; one violet and one blue strand). All techniques were performed by a single investigator. In this study, the suture thread used was #2 ORTHOCORD®, and the passer was an EXPRESSEW® II Flexible Suture Passer (both from Mitek Sports Medicine*; part of the DePuy Synthes Company of Johnson & Johnson).

Four medial suture row patterns of SBT were performed in the following sequence (Fig. 2).

2.3.1. Group 1: Four-hole knotless SBT (n = 10) (Montanez et al., 2016; Wu et al., 2016)

The sutures loaded onto the medial anchors were passed through the tendon 15 mm medial to the edge of the tendon using the passer. There were four perforations in the tendon, and two sutures were inserted into each hole, 9.3 mm apart. All eight suture strands were passed laterally to create a crossing pattern over the tendon. Each lateral anchor received two of the same strands from each medial anchor. The strands were manually tied together with maximum tension.

2.3.2. Group 2: Eight-hole parallel knotless SBT (n = 10) (Lee et al., 2017)

The sutures loaded onto the medial anchors were passed through the tendon 15 mm medial to the edge of the tendon (alternating blue and violet suture strands) using the passer. There were eight perforations in the tendon, and each hole was 4 mm apart. Additionally, there was one suture in each hole. Thereafter, all eight suture strands were passed laterally to create a crossing pattern over the tendon. Each lateral anchor received two of the same strands from each medial anchor. The strands were manually tied together with maximum tension.

2.3.3. Group 3: Eight-hole non-parallel knotless SBT (n = 10)

The sutures from the medial anchors were passed through the tendon 15 mm and 12 mm medial to the edge of the tendon using the passer. There were four perforations in each row. All eight suture strands were passed laterally to create a crossing pattern over the tendon. Each lateral anchor received two of the same strands from each medial anchor. The two strands were manually tied together with maximum tension.

2.3.4. Group 4: Eight-hole knot-tying SBT (n = 10) (Barber et al., 2010)

The sutures from the medial anchors were passed through the tendon in a horizontal mattress fashion 15 mm medial to the edge of the tendon using the same passer. There were eight perforations in the tendon and each hole was 4 mm apart. Additionally, there was one suture in each hole. The four medial mattress stitches were tied with a Fisherman's sliding knot, followed by three half-hitches. Next, one suture from each mattress stitch was pulled laterally to create a crossing pattern over the tendon. Each lateral anchor received two different

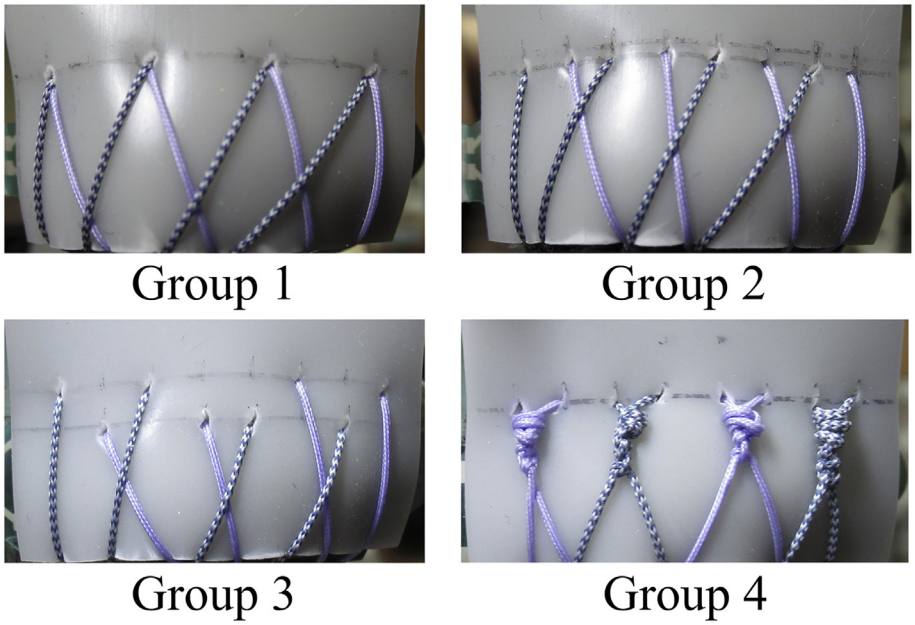

Fig. 2. Four medial row configurations of the suture bridge technique.
Group 1: four-hole knotless suture bridge, Group 2: eight-hole parallel knotless suture bridge, Group 3: eight-hole non-parallel knotless suture bridge, Group 4: eight-hole knot-tying suture bridge.

strands from each medial anchor. The two strands were manually tied together with maximum tension.

2.4. Biomechanical testing

A custom-made cyclic loading machine was used for the biomechanical test. The humerus was placed at an angle of 135° to the vertical axis to mimic the physiological pulling of the tendon, as described in previous studies (Kim et al., 2006; Spang et al., 2009; Wu et al., 2016). The video system was placed at the bursal side of the tendon. The medial end of the tendon model was gripped using custom clamps to prevent slippage. The clamp size was set to 40 mm. A load cell was attached to the upper clamp to record the load (Fig. 3). A custom-made software program on a personal computer was used to control the desired force, the cycle speed, and the number of cycles. First, each model was subjected to a 5 N preload and a cyclic load of 5–30 N at 0.6 mm/s for 20 cycles (Ma et al., 2004; Mihata et al., 2011; Wlk et al., 2015). The tendon model was then subjected to simple tensile loading at 0.6 mm/s until reaching failure (Millett et al., 2017). The assessments recorded the ultimate failure load, the linear stiffness, and the mode of failure. The load and displacement were recorded until failure on a computer using an Instron testing software program. The ultimate failure load was defined as the peak force observed, and the linear stiffness was calculated from the slope of the linear region of the load-displacement curve, after the initial toe region.

2.5. Statistical analyses

Statistical analyses were performed with JMP 13 (SAS Institute., Cary, NC). The values of the ultimate failure load and the linear stiffness are presented as the mean and standard deviation. The Shapiro-Wilk test was used as a test of normality. The ultimate failure load was examined with a one-way analysis of variance, followed by a Tukey-Kramer honest significant difference test. A post-hoc power analysis based on the variance showed a power > 0.85 with $\alpha = 0.05$, if 10 suture constructs per group were tested. The linear stiffness was

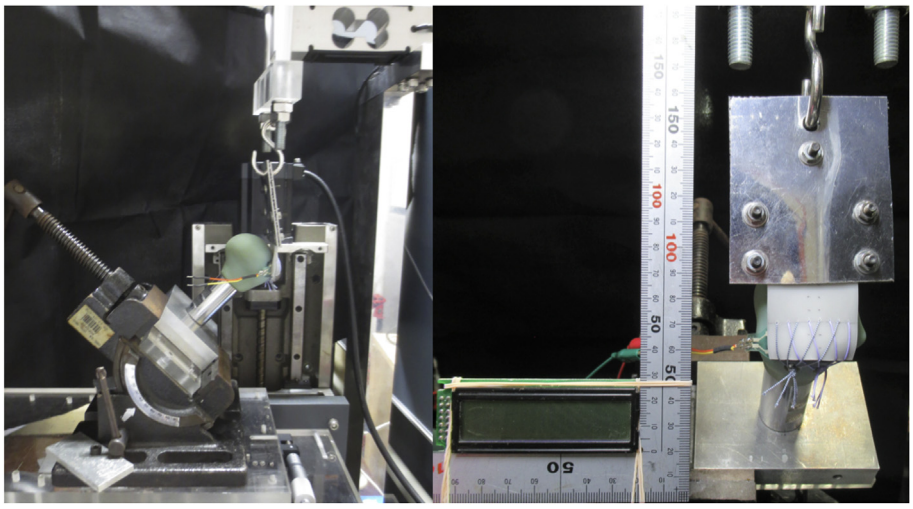

Fig. 3. Custom-made cyclic loading machine. The humerus was placed at an angle of 135° to the vertical axis. Load and displacement were measured by this machine.

Table 1
Results of the ultimate failure load and linear stiffness between the repair techniques.

Repair group	Ultimate failure load (N)		Linear stiffness (N/mm)	
	Mean	SD	Mean	SD
Group 1	129.35	4.25	8.44	0.29
Group 2	160.54*	6.40	9.32‡	0.25
Group 3	138.80**	7.18	8.61	0.31
Group 4	150.21†	9.76	9.72‡	0.40

Ultimate failure load in Group 2 was significantly higher than in other groups. *: $p < 0.05$. Ultimate failure load in Group 3 was significantly higher than in Group 1. **: $p < 0.05$. Ultimate failure load in Group 4 was significantly higher than in Group 1 and Group 3. †: $p < 0.05$. Linear stiffness in Group 2 and Group 4 was significantly higher than in Group 1 and Group 3. ‡: $p < 0.05$.

examined using one-way analysis of variance, followed by a Steel-Dwass test. p values < 0.05 were considered to indicate statistical significance.

3. Results

The ultimate failure load of Group 2 was significantly higher than that in Group 4 ($p = 0.0138$), Group 4 showed a significantly higher failure load in comparison to that in Group 3 ($p = 0.0057$), and Group 3 showed a significantly higher failure load in comparison to that in Group 1 ($p = 0.0276$). The linear stiffness values of Groups 2 and 4 were significantly higher than those of Groups 1 and 3 ($p < 0.05$) (Table 1).

The failure mode of these techniques was consistent with that of a type 2 retear, occurring where the medial row of sutures passed through the rotator cuff and the footprint of the tendon remained attached to the greater tuberosity. Slippage from the clamp or breakage of the screw or the humerus model did not occur.

4. Discussion

Our study demonstrated that the eight-hole parallel knotless SBT (Group 2) had a significantly higher ultimate failure load in comparison to other SBTs. Our results indicated that to achieve a higher tensile strength from suture bridge repair, it is important to reduce the load on each hole through which sutures pass as much as possible. Our results can be explained by the following three interpretations. First, adding more suture-passed holes on the tendon disperses the load such that it does not remain concentrated at one hole. In the present study, only Group 1 had four suture-passed holes on the tendon, and the failure load was significantly lower than that in the other groups. This result is in line with those reported by Maguire et al. and Pauly et al. They described that increasing the number of suture strands across tendon repairs improves the strength of repair by sharing the tensile load (Maguire et al., 2011; Pauly et al., 2011). Therefore, as the number of suture-passed holes increases, the load on each hole decreases, with the load becoming more dispersed, leading to an increase in the ultimate failure load and linear stiffness.

Second, when the numbers of suture-passed holes are equal, aligning the holes along the medial row disperses the load across each hole. Previous reports have not clarified whether the holes through which sutures are inserted must be aligned. Our results showed that all of the holes in Group 2 increased to an equally large size under conditions where a tensile load was applied. In contrast, in Group 3, the four holes which were 15 mm medial from the edge became larger than the four holes which were 12 mm medial from the edge (Fig. 4). This indicates that although the load was dispersed across the eight holes, a larger load was applied to the hole located on the inner side, which eventually led to rupture with a lower ultimate failure load than that in

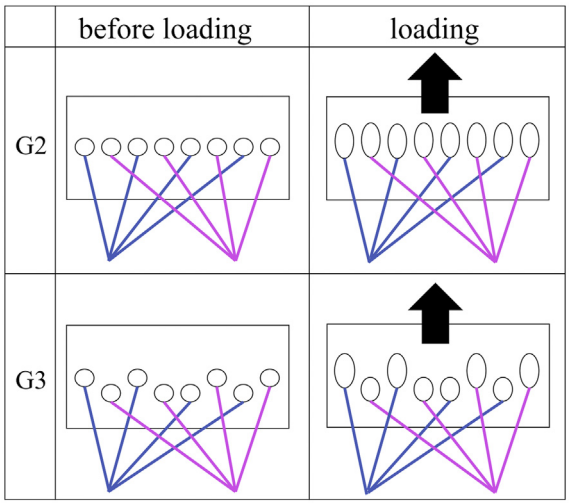

Fig. 4. Comparison of conditions before and after application of the load between Group 2 (G2) and Group 3 (G3): In G2, the eight suture-passed holes became equally large when loaded, whereas in G3, 15-mm medial suture-passed holes showed a greater increase in size than 12-mm medial suture-passed holes in the medial row.

Group 2 (eight-hole parallel knotless SBT). Therefore, when there are equal numbers of suture-passing holes, the failure load and linear stiffness increase with improvement of the alignment of the holes along the medial row.

Third, when the numbers of suture-passed holes are equal, the knotless technique disperses the load across each hole more effectively in comparison to the knot-tying technique. This was revealed by the comparison between Group 2 and Group 4. The result seemed to be affected by the direction of the force vector applied to the hole. In the knot-tying technique, the mattress suture knots were near the holes of the tendon, and the angle between two sutures was larger than that in the knotless technique. When the same load was applied for both techniques, the inward force vectors acting on the next two holes were larger in the knot-tying technique than that in the knotless technique (Fig. 5). The larger inward force vector causes the holes to rupture towards the area between the holes and the two holes tend to combine. This reduces the dispersion of the force on each hole and leads to complete rupture. Thus, in the current study, the larger inward force vector led to the ultimate failure load being lower in the knot-tying technique than in the knotless technique. Numerous reports have compared the strength of knot-tying and knotless SBT (Chu et al., 2011; Leek et al., 2010; Millett et al., 2017; Park et al., 2017; Smith et al., 2017), but there have been no reports that have focused on matching the number of suture-passing holes. Leek et al. and Chu et al. described that the failure load of the knot-tying SBT was significantly higher than that of the knotless SBT (Chu et al., 2011; Leek et al., 2010). However, in these studies, the number of suture-passing holes was different; the knot-tying SBT had four holes in the tendon, while the knotless SBT had two holes. These studies were similar to our study in comparing Group 4 with Group 1. If these previous studies had matched the number of suture-passing holes, the results may have been different.

In the current study, we used artificial materials for comparing the strength of different suture constructs. Many biomechanical studies have compared the suture tensile strength of suture bridge repair using biomaterials. However, because of their individual differences, biomaterials might not allow the accurate comparison of the tensile strength of suture constructs. The advantage of the methodology used in the present study is the uniformity of the biomechanical tests. We unified all factors that might have affected the outcome of this study, except for the design of suture configurations along the medial row; the size, shape, and quality of the rotator cuff or humerus bone, the surgical

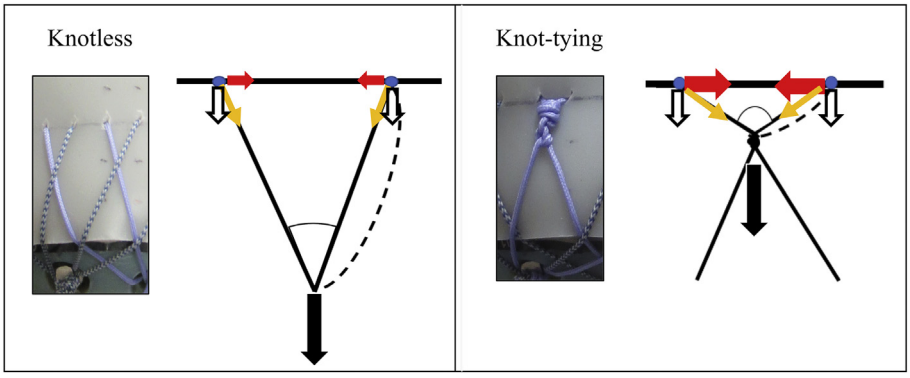

Fig. 5. Comparison of Group 2 and Group 4. When the same load (black arrow) was applied to the two sutures, the tension on the holes (yellow arrow) in the knot-tying SB was larger than that in the knotless SB. The tension on the holes was then dispersed along an inward vector (red arrow) and downward vector (outlined arrow). In this case, the tension along the downward vector is the same, but that along the inward vector in the knot-tying SB is much higher than that in the knotless SB. (For interpretation of the references to colour in this figure legend, the reader is referred to the web version of this article.)

instruments, number of sutures, anchors position, and the size of suture-passed holes. The mode of failure after rotator cuff repair was also the same; in the present study, all post-repair failures during the tensile test were type 2 retears. Thus, the only variable in this study was the medial row configurations of the SBT. Consequently, there was a low standard deviation, ranging from 4.25 to 9.76 N. Accordingly, we used artificial materials to ensure the uniformity, repeatability, and accuracy of the study. We believe that our results might help reduce the rate of type 2 retears after rotator cuff repair.

This study has several limitations. First, we did not use actual rotator cuff tendons and bones. The composition of the artificial materials, as well as that of the animals or cadaveric samples, differed. Of note, the artificial materials had absolute variables that were different from human tendons because of the difference in the materials. Thus, our study showed the relative differences in the ultimate tensile strength and stiffness. Second, this biomechanical study investigated only the initial strength immediately after rotator cuff repair and could not assess the effects of biological factors, such as tendon healing. Third, the present study did not consider the influence of the increased number of holes on the tendon tissue. Further research will be needed to investigate the suitable number of suture-passing holes for each tear size at the clinical level or using animal models. Finally, we did not investigate the contact area or compression force between the tendon and the greater tuberosity during the test.

5. Conclusion

Our results showed that the eight-hole parallel knotless SBT had the highest tensile strength. This study explained the method for dispersing the tensile force and decreasing the load to each hole along the medial row. Thus, it is expected that our study, and the method described, will help reduce the prevalence of type 2 retears after suture bridge repair.

Declaration of Competing Interest

None.

Acknowledgments

We would like to acknowledge Junji Kishimoto, PhD for providing excellent statistical advice. We also acknowledge Raita Miyaji and Chika Miyaji for their technical help.

Funding

This research did not receive any specific grant from funding agencies in the public, commercial, or not-for-profit sectors.

References

Anderl, W., Heuberer, P.R., Laky, B., Kriegleder, B., Reihsner, R., Eberhardsteiner, J., 2012. Eberhardsteiner J. Superiority of bridging techniques with medial fixation on initial strength. Knee Surg. Sports Traumatol. Arthrosc. 20, 2559–2566. https://doi.org/10.1007/s00167-012-1922-9.

Awwad, G.E., Eng, K., Bain, G.I., McGuire, D., Jones, C.F., 2014. Medial grasping sutures significantly improve load to failure of the rotator cuff suture bridge repair. J. Shoulder Elb. Surg. 23, 720–728. https://doi.org/10.1016/j.jse.2013.08.004.

Barber, F.A., Herbert, M.A., Schroeder, F.A., Aziz-Jacobo, J., Mays, M.M., Rapley, J.H., 2010. Biomechanical advantages of triple-loaded suture anchors compared with double-row rotator cuff repairs. Arthroscopy 26, 316–323. https://doi.org/10.1016/j.arthro.2009.07.019.

Bedeir, Y.H., Schumaier, A.P., Abu-Sheasha, G., Grawe, B.M., 2019. Type 2 retear after arthroscopic single-row, double-row and suture bridge rotator cuff repair: a systematic review. Eur. J. Orthop. Surg. Traumatol. https://doi.org/10.1007/s00590-018-2306-8.

Cho, N.S., Yi, J.W., Lee, B.G., Rhee, Y.G., 2010. Retear patterns after arthroscopic rotator cuff repair. Am. J. Sports Med. 38, 664–671. https://doi.org/10.1177/0363546509350081.

Chu, T., McDonald, E., Tufaga, M., Kandemir, U., Buckley, J., Ma, C.B., 2011. Comparison of completely knotless and hybrid double-row fixation systems: a biomechanical study. Arthroscopy 27, 479–485. https://doi.org/10.1016/j.artro.2010.09.015.

Deolio, J.K., Cofield, R.H., 1984. Results of a second attempt at surgical repair of a failed initial rotator-cuff repair. J. Bone Joint Surg. Am. 66, 563–567.

Gartsman, G.M., Drake, G., Edwards, T.B., Elkousy, H.A., Hammerman, S.M., O' Connor, D.P., Press, C.M., 2013. Ultrasound evaluation of arthroscopic full-thickness supraspinatus rotator cuff repair: single-row versus double-row suture bridge (transosseous equivalent) fixation. Results of a prospective, randomized study. J. Shoulder Elb. Surg. 22, 1480–1487. https://doi.org/10.1016/j.jse.2013.06.020.

Goschka, A.M., Hafer, J.S., Reynolds, K.A., Aberle 2nd, N.S., Baldini, T.H., Hawkins, M.J., McCarty, E.C., 2015. Biomechanical comparison of traditional anchors to all-suture anchors in a double row rotator cuff repair cadaver model. Clin. Biomech. 30, 808–813. https://doi.org/10.1016/j.clinbiomech.2015.06.009.

Hein, J., Reilly, J.M., Chae, J., Maerz, T., Anderson, K., 2015. Retear rates after arthroscopic single-row, double-row, and suture bridge rotator cuff repair at a minimum of 1 year of imaging follow-up: a systematic review. Arthroscopy 31, 2274–2281. https://doi.org/10.1016/j.arthro.2015.06.004.

Itoi, E., Berglund, L.J., Grabowski, J.J., Schultz, F.M., Growney, E.S., Morrey, B.F., An, K.N., 1995. Tensile properties of the supraspinatus tendon. J. Orthop. Res. 13, 578–584. https://doi.org/10.1002/jor.1100130413.

Kim, D.H., Elattrache, N.S., Tibone, J.E., Jun, B.J., DeLaMora, S.N., Kvitne, R.S., 2006. Biomechanical comparison of a single-row versus double-row suture anchor technique for rotator cuff repair. Am. J. Sports Med. 34, 407–414. https://doi.org/10.1177/0363546505281238.

Kim, K.C., Shin, H.D., Lee, W.Y., 2012a. Repair integrity and functional outcomes after arthroscopic suture-bridge rotator cuff repair. J. Bone Joint Surg. Am. 94, e48. https://doi.org/10.2106/JBJS.K.00158.

Kim, K.C., Shin, H.D., Lee, W.Y., Han, S.C., 2012b. Repair integrity and functional outcome after arthroscopic rotator cuff repair: double-row versus suture-bridge technique. Am. J. Sports Med. 40, 294–299. https://doi.org/10.1177/0363546511425657.

Kim, K.C., Shin, H.D., Lee, W.Y., Yeon, K.W., Han, S.C., 2018. Clinical outcomes and repair integrity of arthroscopic rotator cuff repair using suture-bridge technique with or without medial tying: prospective comparative study. J. Orthop. Surg. Res. 13, 212. https://doi.org/10.1186/s13018-018-0921-z.

Lee, S.H., Kim, J.W., Kim, T.K., Kweon, S.H., Kang, H.J., Park, J.S., 2017. Is the arthroscopic suture bridge technique suitable for full- thickness rotator cuff tears of any size? Knee Surg. Sports Traumatol. Arthrosc. 25, 2138–2146. https://doi.org/10.1007/s00167-016-4415-4.

Leek, B.T., Robertson, C., Mahar, A., Pedowitz, R.A., 2010. Comparison of mechanical stability in double-row rotator cuff repairs between a knotless transtendon construct versus the addition of medial knots. Arthroscopy 26, S127–S133. https://doi.org/10.1016/j.artro.2010.02.035.

Ma, C.B., MacGillivray, J.D., Clabeaux, J., et al., 2004. Biomechanical evaluation of

arthroscopic rotator cuff stitches. J. Bone Joint Surg. Am. 86, 1211–1216.
Maguire, M., Goldberg, J., Bokor, D., Bertollo, N., Pelletier, M.H., Harper, W., Walsh, W.R., 2011. Biomechanical evaluation of four different transosseous-equivalent/suture bridge rotator cuff repairs. Knee Surg. Sports Traumatol. Arthrosc. 19, 1582–1587. https://doi.org/10.1007/s00167-011-1436-x.
Mihata, T., Fukuhara, T., Jun, B.J., Watanabe, C., Kinoshita, M., 2011. Effect of shoulder abduction angle on biomechanical properties of the repaired rotator cuff tendons with 3 types of double-row technique. Am. J. Sports Med. 39, 551–556. https://doi.org/10.1177/0363546510388152.
Millett, P.J., Espinoza, C., Horan, M.P., Ho, C.P., Warth, R.J., Dornan, G.J., Christoph Katthagen, J., 2017. Predictors of outcomes after arthroscopic transosseous equivalent rotator cuff repair in 155 cases: a propensity score weighted analysis of knotted and knotless self-reinforcing repair techniques at a minimum of 2 years. Arch. Orthop. Trauma Surg. 137, 1399–1408. https://doi.org/10.1007/s00402-017-2750-7.
Montanez, A., Makarewich, C.A., Burks, R.T., Henninger, H.B., 2016. The medial stitch in transosseous-equivalent rotator cuff repair: vertical or horizontal mattress? Am. J. Sports Med. 44, 2225–2230. https://doi.org/10.1177/0363546516648680.
Neyton, L., Godeneche, A., Nove-Josserand, L., Carrillon, Y., Clechet, J., Hardy, M.B., 2013. Arthroscopic suture-bridge repair for small to medium size supraspinatus tear: healing rate and retear pattern. Arthroscopy 29, 10–17. https://doi.org/10.1016/j.arthro.2012.06.020.
Park, M.C., Elattrache, N.S., Ahmad, C.S., Tibone, J.E., 2006. “Transosseous-equivalent” rotator cuff repair technique. Arthroscopy 22, 1360 e1–5. https://doi.org/10.1016/j.arthro.2006.07.017.
Park, J.Y., Siti, H.T., Keum, J.S., Moon, S.G., Oh, K.S., 2010. Does an arthroscopic suture bridge technique maintain repair integrity?: a serial evaluation by ultrasonography. Clin. Orthop. Relat. Res. 468, 1578–1587. https://doi.org/10.1007/s00402-013-1872-9.
Park, M.C., Peterson, A., Patton, J., McGarry, M.H., Park, C.J., Lee, T.Q., 2014. Biomechanical effects of a 2 suture-pass medial inter-implant mattress on transosseous-equivalent rotator cuff repair and considerations for a “technical efficiency ratio”. J. Shoulder Elb. Surg. 23, 361–368. https://doi.org/10.1016/j.jse.2013.06.019.
Park, M.C., Peterson, A.B., McGarry, M.H., Park, C.J., Lee, T.Q., 2017. Knotless transosseous-equivalent rotator cuff repair improves biomechanical self-reinforcement without diminishing footprint contact compared with medial knotted repair. Arthroscopy 33, 1473–1481. https://doi.org/10.1016/j.arthro.2017.03.021.
Pauly, S., Kieser, B., Schill, A., Gerhardt, C., Scheibel, M., 2010. Biomechanical comparison of 4 double-row suture-bridging rotator cuff repair techniques using different medial-row configurations. Arthroscopy 26, 1281–1288. https://doi.org/10.1016/j.arthro.2010.02.013.
Pauly, S., Fiebig, D., Kieser, B., Albrecht, B., Schill, A., Scheibel, M., 2011. Biomechanical comparison of four double-row speed-bridging rotator cuff repair techniques with or without medial or lateral row enhancement. Knee Surg. Sports Traumatol. Arthrosc. 19, 2090–2097. https://doi.org/10.1007/s00167-011-1517-x.
Sano, H., Ishii, H., Yeadon, A., et al., 1997. Degeneration at the insertion weakens the tensile strength of the supraspinatus tendon: a comparative mechanical and histologic study of the bone-tendon complex. J. Orthop. Res. 15, 719–726. https://doi.org/10.1002/jor.1100150514.
Smith, G.C.S., Bouwmeester, T.M., Lam, P.H., 2017. Knotless double-row Suture Bridge rotator cuff repairs have improved self-reinforcement compared with double-row Suture Bridge repairs with tied medial knots: a biomechanical study using an ovine model. J. Shoulder Elb. Surg. 26, 2206–2212. https://doi.org/10.1016/j.jse.2017.06.045.
Spang, J.T., Buchmann, S., Brucker, P.U., Kouloumentas, P., Obst, T., Schroder, M., Burgkart, R., Imhoff, A.B., 2009. A biomechanical comparison of 2 transosseous-equivalent double-rotator cuff repair techniques using bioabsorbable anchors: cyclic loading and behavior. Arthroscopy 25, 872–879. https://doi.org/10.1016/j.arthro.2009.02.023.
Wlk, M.V., Abdelkafy, A., Hexel, M., Krasny, C., Aigner, N., Meizer, R., Landsiedl, F., 2015. Biomechanical evaluation of suture-tendon interface and tissue holding of three suture configurations in torn and degenerated versus intact human rotator cuffs. Knee Surg. Sports Traumatol. Arthrosc. 23, 386–392. https://doi.org/10.1007/s00167-014-2988-3.
Wu, Z., Zhang, C., Zhang, P., Chen, T., Chen, S., Chen, J., 2016. Biomechanical comparison of modified suture bridge using rip-stop versus traditional suture bridge for rotator cuff repair. Biomed. Res. Int. 2016, 9872643. https://doi.org/10.1155/2016/9872643.
Zhang, T., Hatta, T., Thoreson, A.R., Lu, C., Steinmann, S.P., Moran, S.L., Zhao, C., 2018. Rotator cuff repair with a novel mesh suture: an ex vivo assessment of mechanical properties. J. Orthop. Res. 36, 987–992. https://doi.org/10.1002/jor.23668.